Proceedings of the Tenth Pacific Conference on Earthquake Engineering
Building an Earthquake-Resilient Pacific
6-8 November 2015, Sydney, Australia

Analytical modelling of strain penetration deformation in reinforced concrete members

A.H. Altheeb, A.S. Albidah & N.T.K. Lam

Department of Infrastructure Engineering, The University of Melbourne, Parkville, Australia.

J.L. Wilson

Faculty of Science, Engineering and Technology, Swinburne University of Technology, Hawthorn, Australia.

ABSTRACT:

The lateral drift capacity of vertical reinforced concrete elements (e.g. columns and walls) cannot be precisely modelled without considering the four predominant deformation mechanisms: strain penetration, flexure, shear, and sliding shear. Contributions from each mechanism are highly dependent on factors such as shear span ratio, reinforcement ratio, steel mechanical properties, and concrete compressive strength. This paper summarises results from a series of miniature experimentations that was undertaken to study the localization of strains surrounding a preformed crack on a lightly reinforced concrete element. The development of strains on the reinforcement in the plastic hinge range region up to the limit of rupture was of particular interests. A rational strain penetration model has been developed and evaluated by comparisons with results from experimental measurements and with predictions from other analytical models as reported in the literature. The model introduced herein features simplicity of use and precision on slip displacement (Δ_{slip}) estimation.

1 INTRODUCTION

In the event of major earthquakes, vertical elements (e.g. walls and columns) are encouraged to undergo lateral drift in order to sustain imposed lateral displacement before reaching the collapse limit state. The total drift capacity (Δ_{total}) is made up of two components: elastic (Δ_e) and plastic (Δ_p). Typically, a substantial contribution comes from the plastic rotation (i.e. plastic component) where multiple cracks and plasticity extend along the plastic hinge length (L_p) of an element. In addition, a gap opening (Δ_{slip}) at the base may be induced due to flexural reinforcement slippage resulting in magnification of rigid-body rocking in the element.

However, this might not be the case in non-ductile and lightly reinforced elements where the formation of a significant plastic hinge is constrained. Rather, a single major crack is expected to form near the element–foundation interface and hence, would attract most of the plastic rotation (Davey & Blaikie 2005). This situation can be attributed to the fact that the concrete cracking bending moment is greater than the section's ultimate bending capacity. Therefore, the higher the concrete compressive strength, the more likely is the failure of the single-crack brittle mode in a lightly reinforced concrete element. A study by Henry (2013) shows that the risk of this mode of failure could be reduced by increasing the axial load ratio ($n=P/(A_g.f`_c)$).

A series of 37 specimens representing typical structural walls in medium-rise buildings were investigated (Wood 1989). Premature failure at a lateral drift limit of $\leq 2\%$ was perceived to be caused by fracture of the longitudinal rebars in the vicinity of the plastic hinge region in a lightly reinforced concrete wall. Good agreement was found between the experimental results and the observations from a filed reconnaissance survey in the aftermath of the 1985 Chilean earthquake. The vulnerability of the structural walls to brittle mode of failure was aggravated as the flexural reinforcement ratio ($\rho_{vertical}$) was less than 1% (Wood 1989). Similarly, single-crack mode of failure occurred in a number of structural walls forming part of the lateral load-resisting system of a medium or high-rise building, in the 2010/2011 Canterbury earthquakes (Patel, Van & Henry 2014).

Contributions from each of the deformation mechanisms are highly dependent on several factors. However, generally speaking, flexural and strain penetration mechanisms are found to be more dominant in slender elements (e.g. H/L $\geq$ 3 for structural walls), whereas shear and sliding shear mechanisms are more dominant in squat elements (e.g. H/L $\leq$ 1.5 for structural walls). For instance, strain penetration is found to account for as much as 25% of the total lateral displacement of slender lightly reinforced column specimens (Rodsin et al. 2004; Wibowo 2012), and 10% to 20% of the total lateral displacement in slender shear wall specimens (Johnson 2007).

An experimental program was undertaken to investigate the development of strain penetration mechanism in concrete element specimens representing typical loading and boundary conditions in lightly reinforced elements (e.g. columns and walls). In this paper, the local bond stress-strain-slip relationships were analytically modelled based on extensive experimental testing. The developed models were then evaluated by comparisons with predictions from other analytical models (Alsiwat & Saatcioglu 1992; Engstrom 1992; Otani & Sozen 1972; Priestley & Paulay 2002; Sezen & Moehle 2004).

2 EXPERIMENTAL PROGRAM

Ten reinforced concrete element specimens were deliberately designed and loaded to simulate typical segments of lightly reinforced members at the element–foundation interface. The two parameters of particular interest were the reinforcing bar diameter (d_b) and the concrete compressive strength ($f`_c$), as summarised in Table 1.

Table 1. List of Tested Specimens.

Specimen	Bar Dia. (mm)	f`c (MPa)	Limit State			Comments
			Yield	Ultimate	Rupture	
N10#A	10	40.6	√	√	√	
N10#B	10	29	√	√	√	
N10#5	10	64.81	√	√	√	
N10#6	10	52.14	–	–	–	Corrupted
N12#3	12	64.81	–	√	√	Boundaries wrapped with FRP sheets
N12#4	12	52.14	√	–	–	
N12#7	12	47	√	√	√	
N16#1	16	64.81	√	–	–	Boundaries wrapped with FRP sheets
N16#2	16	52.14	√	–	–	
N16#8	16	47	√	–	–	

The specimens were subjected to cyclic (up to yield) and monotonic (post–yield) loading until either the bar fractured or another crack in addition to the preformed notch occurred (Fig. 1). For further details on the experimental apparatus and procedure, refer to the companion paper (Altheeb et al. 2013). The three limit states of particular interest were at yield, ultimate and rupture. The ultimate limit state corresponds to the point of maximum force resistance before drastic degradation begins.

3 ANALYTICAL MODELLING

Precise modelling of non-linear deformations is required to obtain reliable predictions, which may also demand computationally expensive calculations; while overly simplified modelling may compromise accuracy. A number of researchers have investigated the bond-slip relationship of deformed bars utilizing extensive modelling approaches (e.g. Eligehausen, Popov & Bertero 1982; Russo, Zingone & Romano 1990). Others have proposed simpler and more convenient approaches in which the steel

strain profile would comprise regular geometries over the strain penetration length (e.g. Engstrom 1992; Otani & Sozen 1972; Priestley & Paulay 2002; Sezen & Moehle 2004). Otani and Sozen's approach features simplicity of use, where one triangular-shaped strain profile is postulated up to the ultimate limit state. This approach has been found to be appropriate in the elastic region but unduly under-predicting slip in the post-yield region. Alsiwat and Saatcioglu (1992), on the other hand, proposed a more detailed approach in which the strain profile consists of one elastic region and three plastic sub-regions. This approach showed good agreement with the experimental results, although less convenient to use.

The analytical model established in the present study is based on the fact that strain penetration deformation may comprise up to three limit states: elastic, ultimate and rupture. Details of the former two limit states are only provided herein.

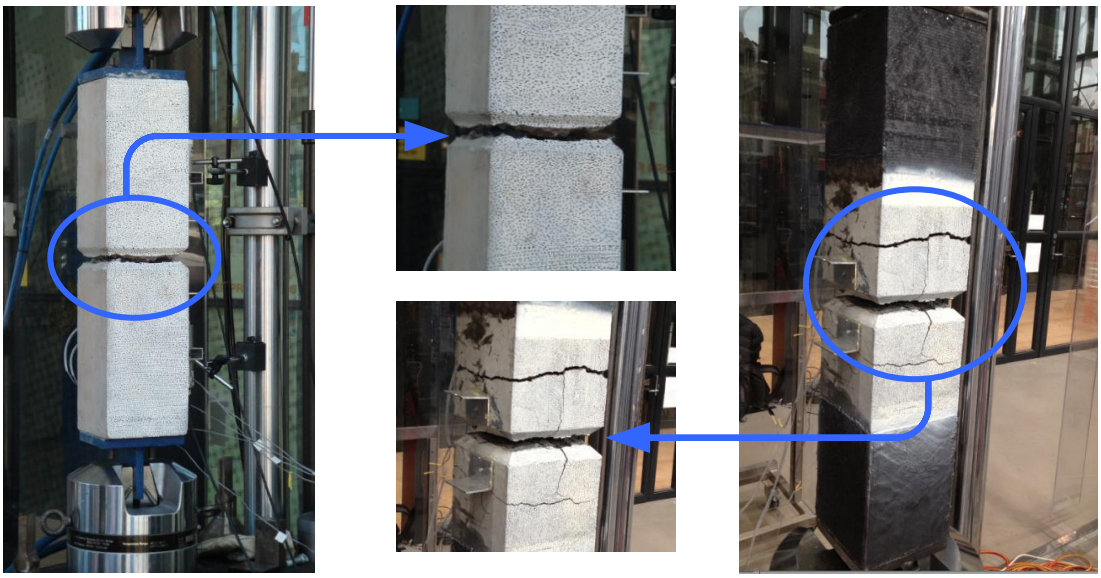

(a) (b)

Figure 1. Specimen testing terminated at: (a) bar fracture with a single crack; (b) formation of multiple cracks.

3.1 **Yield limit state (elastic region)**

From the laboratory test results and the aforementioned studies, we realize that Δ_{slip} is highly dependent on such factors as concrete compressive strength ($f`_c$), bar diameter (d_b), bar ductility (μ) and applied stress (f_s). The elastic slip displacement ($\Delta_{slip,elastic}$) can best be represented by a triangular-shaped strain profile, and hence, can be readily obtained by integrating the area under the curve. The steel stress/strain is highest at the crack tip and begins to fade along a distance (L_s) from the crack tip (Fig. 2).

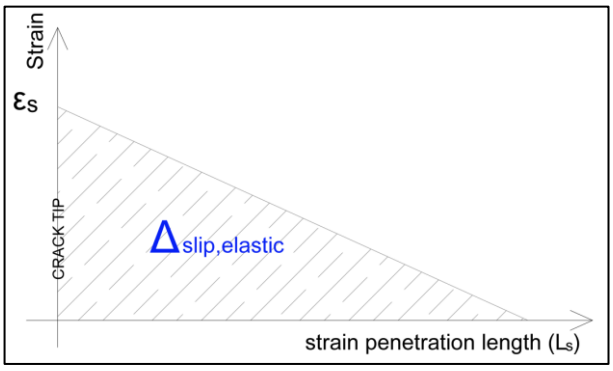

Figure 2. Typical strain profile in the elastic region.

$$\Delta_{slip,elastic} = 2\int_0^L \varepsilon_s dx = 2\left(\frac{1}{2}\varepsilon_s \cdot L_s\right) \quad (1)$$

$$\varepsilon_s = \frac{f_s}{E_s}; \qquad \varepsilon_s \le \varepsilon_y \quad (2)$$

The elastic strain penetration length (L_s) can be computed assuming uniform elastic bond stress (u_e) and equilibrium between applied (F_s) and resistant (F_{bond}) forces on the bar as follows:

$$F_s = f_s \cdot A_{bar} = f_s \cdot \frac{\pi d_b^2}{4} \quad (3)$$

$$F_{bond} = u_e \cdot \pi d_b \cdot L_s \quad (4)$$

$$\therefore\ L_s = \frac{f_s d_b}{4u_e} \quad (5)$$

Table 2. Analytical models of the elastic strain penetration displacement.

Researcher(s)	Model	Comment / Strain Profile
Engstrom (1992)	$\Delta_y = 0.576\left(\frac{d_b f_{sy}^2}{2.5\sqrt{f_c'} \cdot E_s}\right)^{0.714} + \frac{4d_b f_{sy}}{E_s}$	Good bond conditions
Engstrom (1992)	$\Delta_y = 0.576\left(\frac{d_b f_{sy}^2}{1.25\sqrt{f_c'} \cdot E_s}\right)^{0.714} + \frac{4d_b f_{sy}}{E_s}$	All other cases
Alsiwat and Saatcioglu (1992)	$L_s = \frac{f_s}{f_y} \times \max\left(300, \frac{440 f_y \pi d_b}{4800\sqrt{f_c'}}\right)$	
Sezen and Moehle (2004)	$L_s = \frac{f_s d_b}{4\sqrt{f_c'}}$	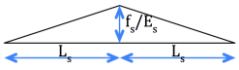
Otani and Sozen (1972)	$L_s = \frac{f_s d_b}{4 \times 0.54\sqrt{f_c'}}$	
Priestley and Paulay (2002)	$L_s = \frac{4400 f_{sy} d_b}{E_s}$	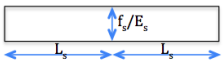
The present study	$L_s = \frac{f_s d_b}{4u_e};\ u_e = 0.3\left(\frac{d_b f_s}{f_y}\right)^{0.5}\sqrt{f_c'}$	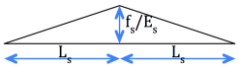

The newly developed analytical model (elastic region) is listed in Table 2 along with several models reported in the literature. Further, all the models have been schematically evaluated by comparisons with laboratory data (Fig. 3-4). The analytical models reported in the literature tend to over-predict the yield slip displacement. However, both the proposed and Sezen & Mohle models are found to match well with the measured displacements.

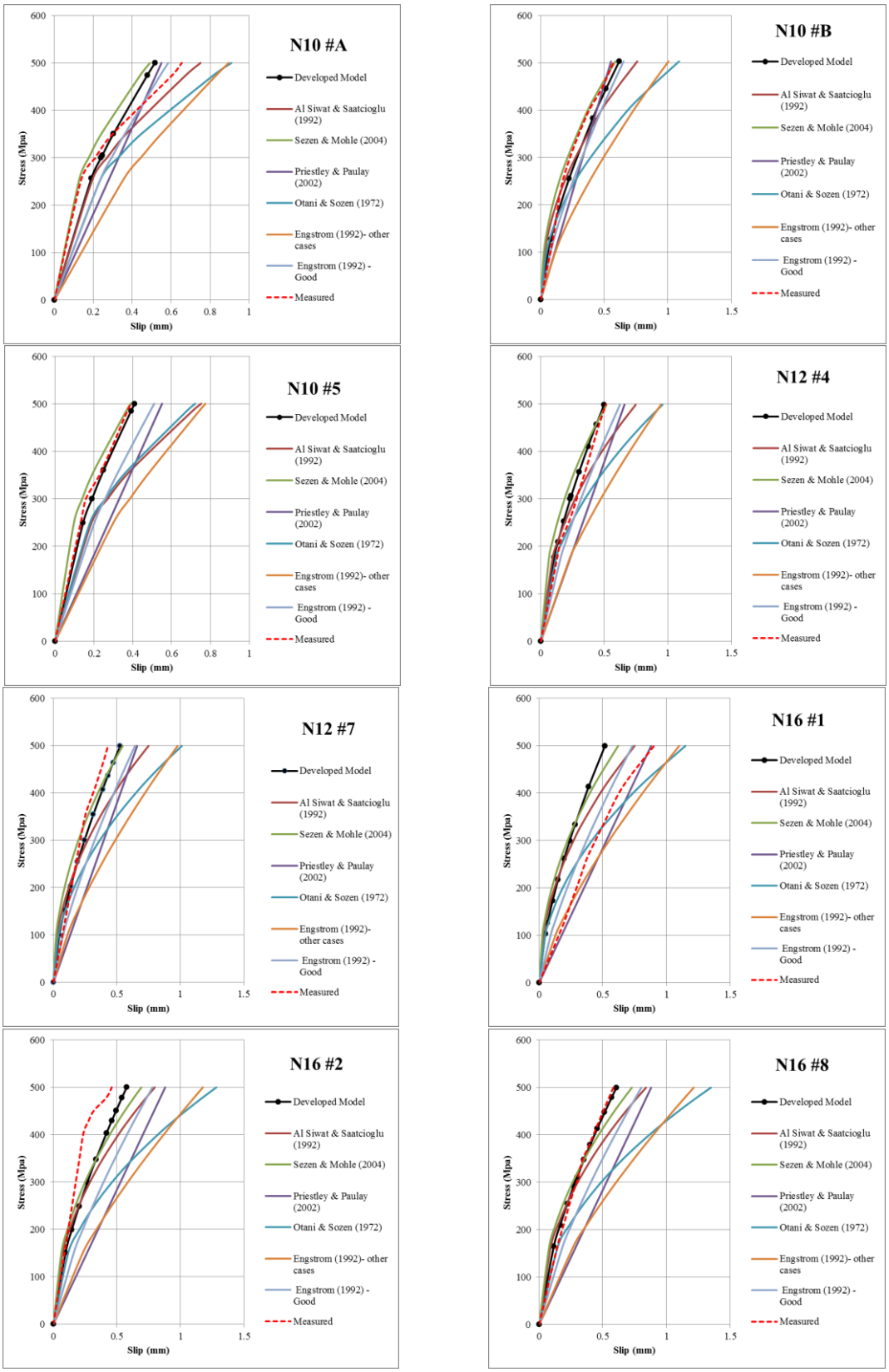

Figure 3. Comparisons of experimental results and analytical predictions for elastic strain penetration.

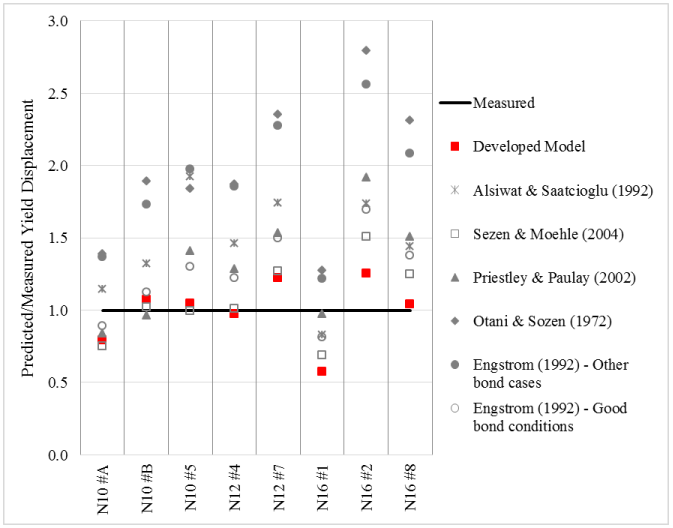

Figure 4. Ratios of predicted to measured strain penetration displacement at the yield limit state.

3.2 **Post-yield limit state (plastic region)**

Similarly, the bond-slip relationship was derived, assuming uniform plastic bond stress (u_p) over the plastic strain penetration length (L_p). When exceeding the bar yielding stress, bond deterioration between the reinforcing steel and concrete is aggravated, resulting in a deeper strain penetration length, and hence, additional slip displacement. Sezen and Moehle (2004), for instance, suggested that the plastic region develops half of the uniform bond stress that can be developed in the elastic region, $0.5\sqrt{f`_c}$ and $\sqrt{f`_c}$, respectively.

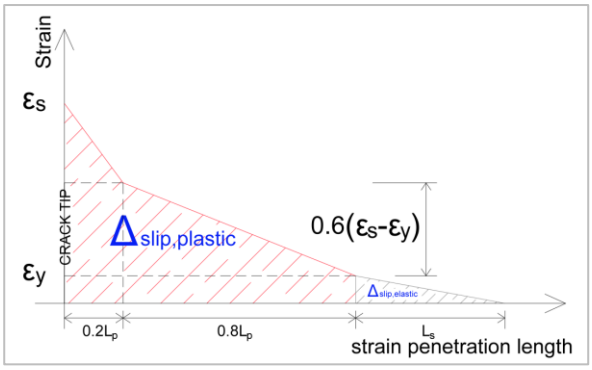

Figure 5. Typical strain profile in the plastic region.

For the sake of the plastic slip displacement ($\Delta_{slip,plastic}$) prediction, both the plastic strain penetration (L_p) and the steel strain profile were modelled (Fig. 5). It should be noted that (L_p) was derived from computationally intensive nonlinear regression analyses on the test results while the proposed steel strain profile was based on the monitored steel strain distribution. Total slip displacement ($\Delta_{slip,total}$) can be determined from Equations 6 through 9:

$$\Delta_{slip,total} = \Delta_{slip,yield} + \Delta_{slip,plastic} \tag{6}$$

$$\Delta_{slip,plastic} = \left[L_p\varepsilon_y + \frac{1.6\left(\varepsilon_s - \varepsilon_y\right)}{2}0.2L_p + \frac{0.6\left(\varepsilon_s - \varepsilon_y\right)}{2}0.8L_p \right] \times 2 \tag{7}$$

$$\Delta_{slip,plastic} = \left(0.8\varepsilon_s + 1.2\varepsilon_y\right)L_p \tag{8}$$

where

$$L_p = \frac{(f_s - f_y)d_b^{1.2}}{4\sqrt{f_c'}}; \qquad \varepsilon_y \le \varepsilon_s \le \varepsilon_u \tag{9}$$

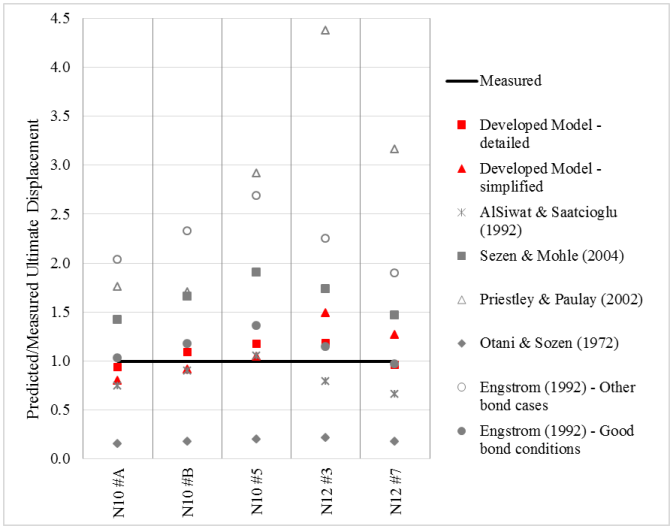

Figure 6. Ratios of predicted to measured strain penetration displacement at the ultimate limit state.

A comparison in Figure 6 shows that the ultimate slip displacement prediction from the model developed herein agrees well with the experimental results. It also corresponds to a more elaborate analytical model (i.e. Alsiwat and Saatcioglu1992).

3.3 **Worked example**

The application of the proposed analytical models is presented in this illustrative worked example. A lightly reinforced concrete shear wall that forms part of the lateral resisting system in a 5-storey building is shown in Figure 7. The wall measures 1.5 m long × 0.15 m wide × 17.50 m high from the base. The wall reinforcement in both directions is provided in the form of a single-layer steel mesh using N10 deformed reinforcing bars at a 200 mm spacing that corresponds to a longitudinal reinforcement ratio of $\rho_{longitudinal}$ = 0.25%. The experimentally evaluated reinforcing steel yield stress is f_y = 500 MPa, the yield strain is ε_y = 0.0025, the ultimate stress is f_{su} = 720 MPa, and the ultimate strain is ε_{su} = 0.10. The concrete compressive strength is $f`_c$ = 40 MPa, and the applied axial load ratio is N = 5%, which would induce an axial force of 450 kN at the wall base.

The yield slip displacement ($\Delta_{slip,yield}$) at which the outermost bar layer reaches the yield strength can be estimated using Equations 1–5, whereas the ultimate slip displacement ($\Delta_{slip,total}$) at which the outermost bar layer reaches the ultimate strength can be estimated using Equations 6–9. Details of the calculations are shown by Equations 10a–10c.

$$\Delta_{slip,yield} = 2\left(\frac{1}{2}\varepsilon_s \cdot L_s\right) = 2\left(\frac{1}{2}\times 0.0025 \times 208\right) = 0.5mm \tag{10a}$$

$$\Delta_{slip,plastic} = (0.8\varepsilon_s + 1.2\varepsilon_y)L_p = (0.8\times 0.10 + 1.2\times 0.0025)137.8 = 11.4mm \tag{10b}$$

$$\Delta_{slip,total} = \Delta_{slip,yield} + \Delta_{slip,plastic} = 0.5 + 11.4 = 11.9mm \tag{10c}$$

The expected lateral displacement ($\Delta_{lateral}$) can then be calculated using Equation 11.

$$\Delta_{lateral} = \frac{\Delta_{slip}}{N.A. - d_{x1}} \cdot H \tag{11}$$

Where $N.A.$is the neutral axis depth, d_{x1} is the distance between the outermost longitudinal bar and the wall side surface, and H is the wall total height. Substituting the numerical values into Equation 11 would result in lateral displacements of:

$$\Delta_{lateral,yield} = \frac{\Delta_{slip,yield}}{N.A. - d_{x1}} \cdot H = \frac{0.5}{1124 - 50} \times 17500 = 8.5mm \quad (12a)$$

$$\Delta_{lateral,ultimate} = \frac{\Delta_{slip,total}}{N.A. - d_{x1}} \cdot H = \frac{11.9}{1195.5 - 50} \times 17500 = 182.7mm \quad (12b)$$

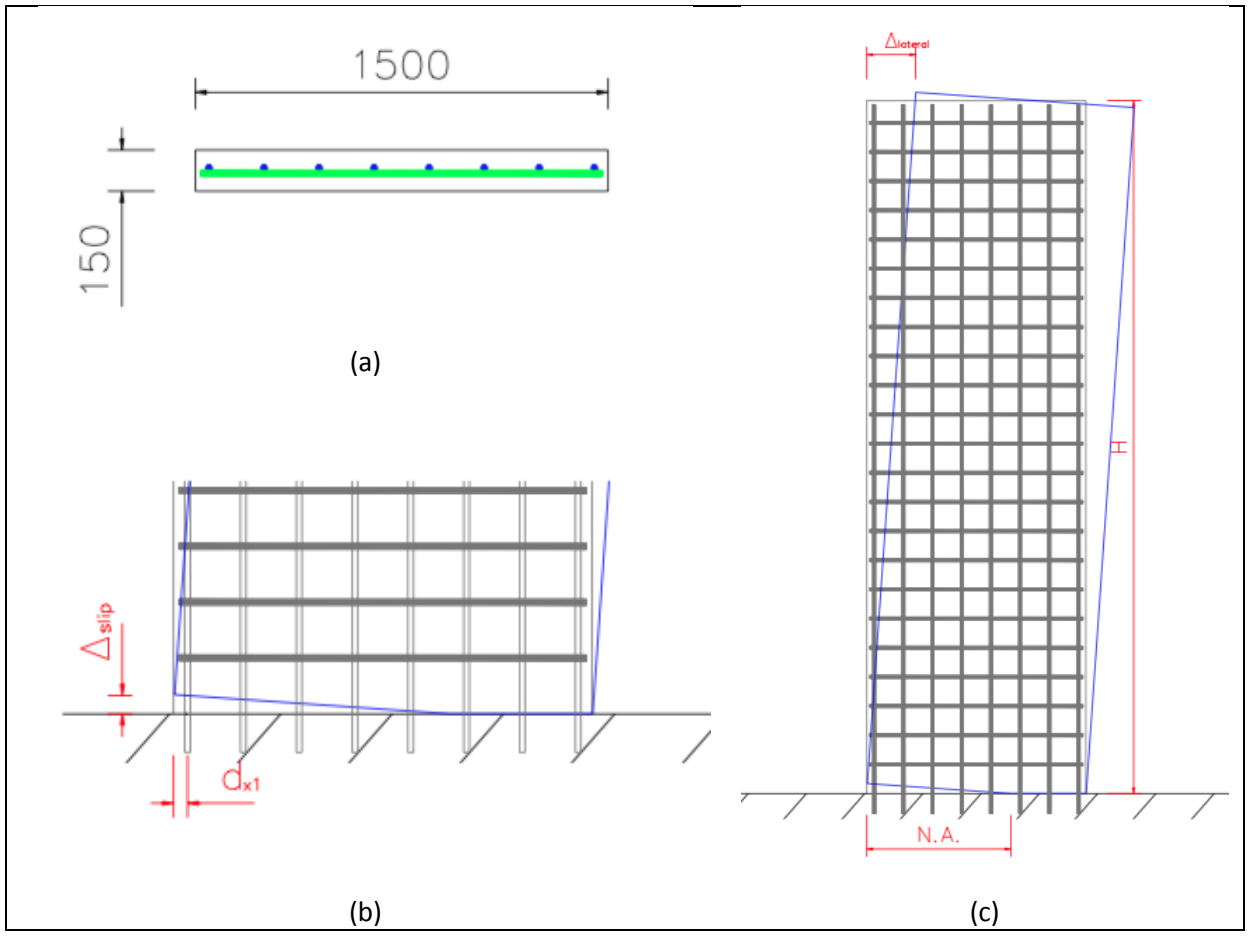

Figure 7. Details of the example wall: a) reinforcement and geometry, b) formation of a single crack at the wall base, and (c) expected deflected shaped.

4 CONCLUSION

In this study, we reported on extensive laboratory testing of a series of miniature specimens. The concrete compressive strength $f`_c$ and reinforcing bar diameter d_b were amongst the parameters investigated. The specimens were thoughtfully designed, detailed and loaded to mimic real loading and boundary conditions, given that only one crack was formed for the majority of specimens reinforced with bars N10 and N12.

Analytical models have been developed for reliable and convenient prediction of strain penetration displacement, with particular emphasis on very lightly reinforced elements, where a single main crack was expected to form in the vicinity of the member's base.

A steel strain profile was rationally modelled in two regions: elastic and plastic. The former consisted of one triangular-shaped geometry, whereas the latter consisted of two trapezoidal-shaped geometries.

REFERENCES:

Alsiwat, JM & Saatcioglu, M 1992, Reinforcement anchorage slip under monotonic loading, *Journal of*

Structural Engineering, Vol 118(9) 2421-38.

Altheeb, A, Albidah, A, Lam, NTK & Wilson, J 2013, The Development of Strain Penetration in Lightly Reinforced Concrete Shear Walls, in *Australian Earthquake Engineering Society 2013 Conference, Hobart, Tasmania, 15-17 November 2013*.

Davey, R & Blaikie, E 2005, On the flexural ductility of very lightly reinforced concrete sections, in *New Zealand Society for Earthquake Engineering Conference*, pp. 11-3.

Eligehausen, R, Popov, EP & Bertero, VV 1982, *Local bond stress-slip relationships of deformed bars under generalized excitations*, UCB-report University of Calfomia, Berkeley.

Engstrom, B 1992, Anchorage of ribbed bars in the post yield stage, in *International Conference on Bond in Concrete, Riga, Latvia*.

Henry, R 2013, Assessment of minimum vertical reinforcement limits for RC walls, *Bulletin of the New Zealand Society for Earthquake Engineering*, Vol 46(2) 88-96.

Johnson, BM 2007, Longitudinal Reinforcement anchorage Detailing effects on RC shear wall Behavior, Master thesis, University of Minnesota.

Otani, S & Sozen, MA 1972, *Behavior of multistory reinforced concrete frames during earthquakes*, University of Illinois Engineering Experiment Station. College of Engineering. University of Illinois at Urbana-Champaign.

Patel, V, Van, B & Henry, R 2014, Effect of reinforcing steel bond on the seismic performance of lightly reinforced concrete walls, in *2014 NZSEE Annual Conference*.

Priestley, M & Paulay, T 2002, What is the stiffness of reinforced concrete walls, *Journal of the Structural Engineering Society New Zealand*, Vol 15(1).

Rodsin, K, Lam, N, Wilson, J & Goldsworthy, H 2004, Shear controlled ultimate behaviour of non-ductile reinforced concrete columns, in *Australian Earthquake Engineering Society Proceedings of the 2004 Conference*.

Russo, G, Zingone, G & Romano, F 1990, Analytical solution for bond-slip of reinforcing bars in RC joints, *Journal of Structural Engineering*, Vol 116(2) 336-55.

Sezen, H & Moehle, JP 2004, Shear strength model for lightly reinforced concrete columns, *Journal of Structural Engineering*, Vol 130(11) 1692-703.

Wibowo, A 2012, Seismic performance of insitu and precast soft storey buildings, PhD thesis, Swinburne University of Technology.

Wood, SL 1989, Minimum tensile reinforcement requirements in walls, *ACI Structural Journal*, Vol 86(5).